LOAD ANALYSIS OF LOOK-AHEAD COLLECTIVE PITCH CONTROL USING LIDAR

D. Schlipf[1], T. Fischer[1], C.E. Carcangiu[2], M. Rossetti[2], E. Bossanyi[3]
[1]Endowed Chair of Wind Energy, Universität Stuttgart, Germany, david.schlipf@ifb.uni-stuttgart.de;
[2]Alstom Wind S.L., Barcelona, Spain; [3]Garrad Hassan Ltd, Bristol, UK

Summary

In a detailed analysis the benefit of LIDAR assisted collective pitch control is evaluated, by using a realistic LIDAR simulator and comparing it to an advanced feedback controller. With the proposed look-ahead controller best load reduction can be observed for high turbulence and high wind speed. Damage equivalent loads on tower and blades are reduced up to 20% and 10%, respectively.

1. Introduction

Nacelle based LIDAR (Light detection and ranging) systems provide preview information of wind disturbances at various distances in front of a wind turbine. Preliminary work towards this objective [1] has shown that the predictive knowledge of the rotor effective wind speed can be used to improve the speed regulation by a predictive feedforward update to the collective pitch feedback controller, which indicates load reduction of tower and blades.
This paper presents a fatigue load analysis to concretize the improvement of look-ahead collective pitch control of a 5MW turbine [2], using realistic LIDAR simulations and comparing the results to the UpWind controller [3].
In this paper the basic idea of the look-ahead controller is presented in Section 2. In Section 3 the optimization of the controller parameter is elaborated and the implementation is described in Section 4. Section 5 shows the results and Section 6 concludes the presented work.

2. Controller concept

The primary control goal of the collective pitch feedback controller Σ_{FB} is to maintain the rated generator speed Ω_{rated} in the presence of varying wind v above the rated wind speed by adjusting the collective pitch angle θ (see Figure 1).

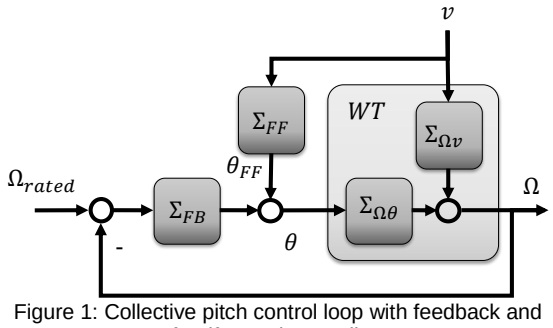

Figure 1: Collective pitch control loop with feedback and feedforward controller.

In theory, a known disturbance like the varying wind can be perfectly compensated by a feedforward controller Σ_{FF}, if the influence on the generator speed of the wind $\Sigma_{\Omega v}$ and the pitch angel $\Sigma_{\Omega\theta}$ is known and $\Sigma_{\Omega\theta}$ is invertible.
Then the update to the feedback output

$$\Sigma_{FF} = -\Sigma_{\Omega\theta}^{-1}\Sigma_{\Omega v} \tag{1}$$

compensates the disturbance entirely. Due to its complexity this perfect compensation cannot be found for an aeroelastic model of a wind turbine and a wind disturbance in form of a stochastic vector field. Therefore in [1] the wind field was reduced to a rotor effective wind speed v_0, and a static compensation was proposed, equivalent to the nonlinear function $\theta_{ss}(v_{ss})$ of the static pitch angle θ_{ss} over static wind speed v_{ss}. Due to the higher relative degree of $\Sigma_{\Omega\theta}$ compared to $\Sigma_{\Omega v}$, it is beneficial to use the value of v_0 shifted with τ_s ahead in time. The static feedforward Σ_{FFs} controller is then

$$\theta_{FFs}(t) = \theta_{ss}\big(v_0(t-\tau_s)\big). \tag{2}$$

Here a dynamic feedforward controller is designed by assuming the following model of the wind turbine:

$$\begin{aligned} J\dot{\Omega} + iM_g &= M_a(\Omega, \theta_e, v_0) \\ \ddot{\theta}_e + 2\xi\omega\dot{\theta}_e + \omega^2(\theta_e - \theta) &= 0, \end{aligned} \tag{3}$$

where M_a is the aerodynamic torque, M_g the electrical generator torque and θ_e the effective blade pitch angle. Moreover, i is the gear box ratio and J is the sum of the moments of inertia about the rotation axis, ω the undamped natural frequency, and ξ the damping factor.
Then the dynamic feedforward controller Σ_{FFd} is

$$\begin{aligned} v_{FF} &= (\ddot{v}_0 + 2\xi\omega\dot{v}_0 + \omega^2 v_0)/\omega^2 \\ \theta_{FFd} &= \theta_{ss}(v_{FF}). \end{aligned} \tag{4}$$

This theoretically would counteract all changes in v_0, because the aerodynamic torque satisfies $M_a(\Omega_{rated}, \theta_{ss}, v_{ss}) = iM_g$. But this system is not proper and therefore has to be combined with a filter. Depending on the filter and model accuracy a better compensation can be expected for Σ_{FFd} compared to Σ_{FFs}, because additional system information is included in the feedforward control.

3. Controller Parameter Optimization

Instead of linear loop shaping techniques for controller parameter optimization an approach to directly estimate standard deviations via a rotor averaged wind spectrum and the closed loop transfer function is proposed.

3.1 Rotor Averaged Kaimal Spectrum

In [4] the Kaimal Spectrum $S_{HH}(f)$ for the hub height wind speed and the coherence $coh(r_{ij}, f)$ for two points with distance r_{ij} are defined.

The rotor averaged spectrum can be derived by an average of the cross and auto spectrum densities of all points and combinations in the rotor plane D:

$$S_0(f) = \iint_D \iint_D \frac{S_{ij}(r_{ij}, f)}{(\pi R^2)^2} dy_j dz_j dy_i dz_i \quad (5)$$

By assuming that there is an average phase of zero between any two points [5], the imaginary parts of the cross spectra can be considered zero. Assuming that the auto spectrum densities in all points are equal, the spectra in (5) result in

$$S_{ij}(f) = coh(r_{ij}, f) S_{HH}(f). \quad (6)$$

In the special case of discrete wind fields such as used for simulations, (5) can be simplified to

$$S_0(f) = \sum_{i=1}^{n} \sum_{j=1}^{n} \frac{coh(r_{ij}, f)}{n^2} S_{HH}(f) \quad (7)$$

where n is the number of grid points.

3.2 Estimated Spectrum of Generator Speed

With rotor averaged linear models for different wind speeds of the controlled turbine, the closed loop transfer function $G_{\Omega v}$ can be calculated including the most important part for the collective pitch controller: The collective pitch controller with gain scheduling, filters for the generator speed, the generator torque controller above rated wind speed trying to maintain constant power and the tower vibration damping.

Along with the rotor averaged Kaimal spectrum (7) for given v_{HH} and σ_{HH} the spectrum of the generator speed can be estimated by

$$S_\Omega(f) = |G_{\Omega v}(f)|^2 S_0(f), \quad (8)$$

and the standard deviation of the generator speed is

$$\sigma(\Omega) = \sqrt{\int_0^\infty S_\Omega(f) df}. \quad (9)$$

Figure 2 shows the estimated spectra and the spectra obtained from simulations with different seeds (v_{HH}=16m/s, σ_{HH}=2.82m/s). For the feedback controller a good correlation can be achieved, although nonlinear and stochastic effects cannot be captured by the estimation. The differences between the estimation and the simulation for the look-ahead controller are a result of non-perfect measurements.

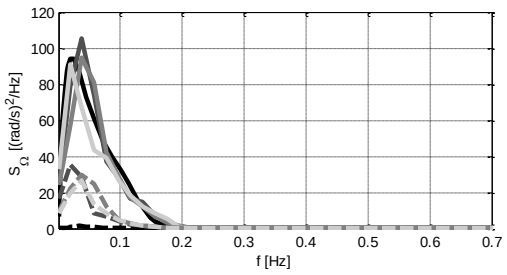

Figure 2: Spectra of the generator speed: (black) estimated, (shades of gray) from simulations, (solid) feedback only, (dashed) look-ahead.

4. Implementation

For a detailed fatigue load analysis for the LIDAR look-ahead controller, the UpWind reference turbine with a monopile in 20m water depth [2] is used.

Measurements of different LIDAR systems are implemented in the aero-elastic tool GH Bladed. A reference controller [3], which includes among others an individual pitch control and a tower vibration damping, is extended by an update from the processed simulated measurements (see Figure 3).

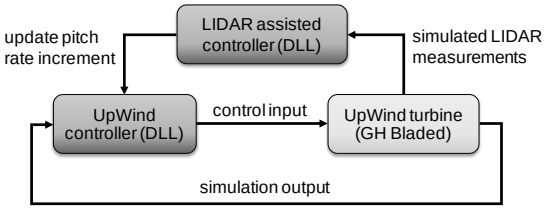

Figure 3: Scope of the implementation of the look-ahead controller assisted by simulated LIDAR measurements.

4.1 Simulation of LIDAR Measurements

To realistically reproduce the LIDAR measurements, the generic wind field used for the aeroelastic simulations is evaluated online in GH Bladed according to the characteristic of a real nacelle based LIDAR system [6]. Taylor's frozen turbulence hypothesis is used, assuming the turbulent wind field to be unaffected when approaching the rotor and moving with average wind speed.

Figure 4 shows the chosen circle scan, which provides twelve measurements each 2s in five distances from 0.5D to 1.5D with the rotor diameter D=126m. The component of the wind vector in laser beam direction (line-of-sight wind speed) is only detected. Volume measurements are considered by calculating the line-of-sight wind speeds for a pulse with the length of 60m at various distances along the laser beam and applying a weighting function [6].

The line-of-sight wind speeds are passed to an external dynamic link library (DLL) which processes the simulated LIDAR measurements and provides the pitch rate increment to the controller DLL.

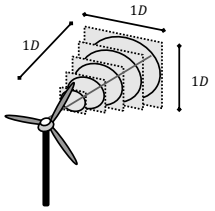

Figure 4: Scope of LIDAR measurements.

4.2 Processing of LIDAR Measurements

The upwind component of the wind is reconstructed using the assumption of perfect alignment with the wind and then averaged for each circle over the last trajectory. The five time series are time shifted according to Taylor's frozen turbulence hypothesis and combined to one wind speed v_0.

The data has to be low pass filtered (cutoff frequency 0.2Hz) in order to account for uncertainties in Taylor's frozen turbulence hypothesis [6]. In the case of the dynamic feedforward controller the filter is combined with (4) to get a realizable system.

4.3 Determination of the Pitch Rate Increment

Notwithstanding Figure 1, an update $\dot{\theta}_{FF}$ to the pitch rate increment was chosen for simplicity in the implementation. Therefore Σ_{FFs} is changed to

$$\dot{\theta}_{FFs}(t) = \dot{v}_0(t-\tau_s)\frac{d\theta_{ss}}{dv_{ss}}\big(v_0(t-\tau_s)\big) \qquad (10)$$

and Σ_{FFd} to

$$\begin{aligned} v_{FF} &= (\ddot{v}_0 + 2\xi\omega\dot{v}_0 + \omega^2 v_0)/\omega^2 \\ \dot{\theta}_{FFs} &= \dot{v}_{FF}\frac{d\theta_{ss}}{dv_{ss}}(v_{FF}). \end{aligned} \qquad (11)$$

The advantage of using $d\theta_{ss}/dv_{ss}$ instead of the derivative of θ_{FF} is, that the transition from below rated to rated wind speed can be easily smoothed out. Figure 5 shows the used $d\theta_{ss}/dv_{ss}$ limited to 5°s/m. With this limit, still higher loads have been observed in the transition region between partial and rated load due to strong changes in the thrust.

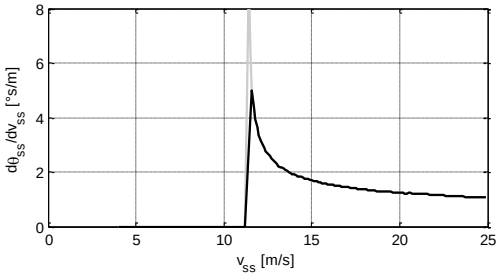

Figure 5: Theoretical (gray) and limited (black) feedforward law $d\theta_{ss}/dv_{ss}$ for the pitch rate increment.

As an example Figure 6 shows the perfect transition (dashed black) in terms of load reduction for the tower base fore-aft bending moment M_{yT}, which would change slowly from the peak value at rated wind speed (at t=306s) to the corresponding value of above rated wind speed (at t>313s).

The look-ahead controller (dark gray) shows a worse behavior than the feedback controller (black). With a limitation of the pitch rate increment (light gray) the damage equivalent loads (DEL) of this 10min simulation show a significant reduction (see Table 1).

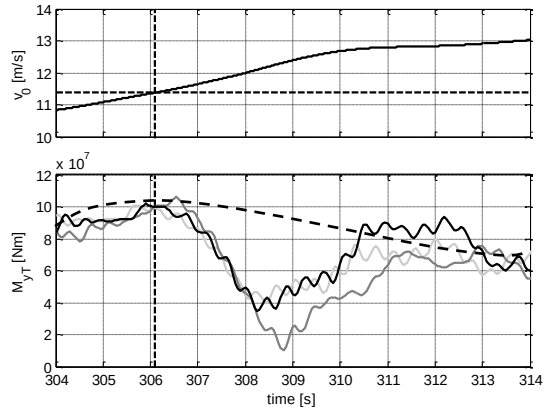

Figure 6: Top: Filtered and time-shifted LIDAR measurement. Bottom: Improvement of the look-ahead controller in the transition region through a limitation of the pitch rate increment (light gray); feedback (black) and look-ahead controller without limitation (dark gray).

Table 1: DEL (m=4, N=2E06) for the complete 10min simulation of Figure 6.

Controller	DEL M_{yT} [MNm]	Changes to Σ_{FB}
Σ_{FB}	94.1	0%
$\Sigma_{FB} + \Sigma_{FFs}$	98.9	+5,1%
$\Sigma_{FB} + \Sigma_{FFs}$ limited	79.6	-15,4%

5. Results

5.1 Optimized Parameter

Considering Section 2, the prediction time for the static feedforward depends only on the pitch actuator dynamics and no additional prediction time is needed for the dynamic feedforward controller. But with the controller parameter optimization over estimated spectra a dependency from the mean wind speed can be observed for both feedforward controllers. Through simulations, slightly better results have been achieved with a longer prediction time, however still depending on the mean wind speed. This investigation has been made for better understanding, because in general the feedforward control is quite robust and for a constant prediction time (1s) the results do not change significantly.

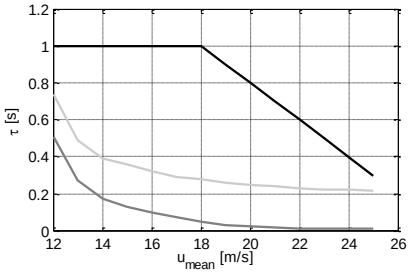

Figure 7: The prediction time from the spectra estimation ($\tau_{s,Spec}$ light gray, $\tau_{d,Spec}$ dark gray) and obtained through optimization via simulations τ_{Sim} (black).

The feedforward relieves the feedback controller. Therefore better results can be expected for a redesigned feedback controller if used along with the feedforward controller. Spectra estimation and simulations affirm this assumption and best results were found for redesigned feedback parameters: half of the previous proportional gain and a quarter of the integral gain. All other parameters of the Upwind feedback controller remained unchanged.

5.2 Results for Fatigue Load Reduction

In the first step various simulations with a Rayleigh distribution (A=12m/s) and wind turbulence class A according to [4] were conducted, to estimate the load reduction potential of the proposed controller for fatigue loads. Bins of 2m/s from 4 to 24 m/s had been chosen, each simulated with 3 different seeds.

The effect of using LIDAR assisted control can be observed clearly in the frequency domain (see Figure 8) for a simulation with v_{HH}=16m/s, σ_{HH}=2.82m/s. The look-ahead controller can significantly reduce the influence of the wind disturbance to rotor speed and to the tower base fore-aft bending moment below the 1P-frequency. Also the pitch rate is reduced in this region.

The standard deviation of the rotor speed and the DEL (m=4, N=2E06, 20 years) over the different wind

speeds can be seen in Figure 9. Both look-ahead controller show improvements to the feedback controller used alone, whereas slightly better results can be achieved with τ_{Sim} compared to $\tau_{s,Spec}$ (Table 2). This indicates a robustness of the feedforward controller with regard to the prediction time. Almost no differences can be observed between the static and the dynamic feedforward due to the low cutoff frequency of the low pass filter.
Moreover several simulations have been run using Rayleigh distributions with A=10m/s and A=12m/s, and wind turbulence class A and B to evaluate the influence of the wind distribution and the turbulence on the performance of LIDAR assisted control, see Table 3. The best reduction is achieved for high wind speeds. The wind turbine class affects the blade out-of-plane root bending moments M_{yB} while no significant effects on other loads can be observed.

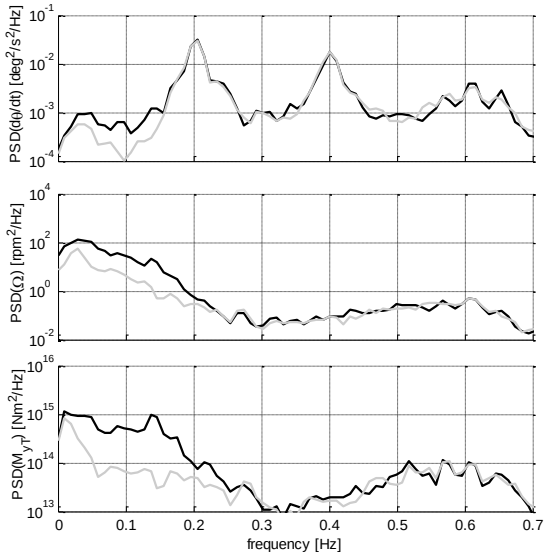

Figure 8: Power spectral density of pitch rate, rotor speed and tower base fore-aft bending moment, feedback controller only (black) and look-ahead (τ_{Sim}, gray).

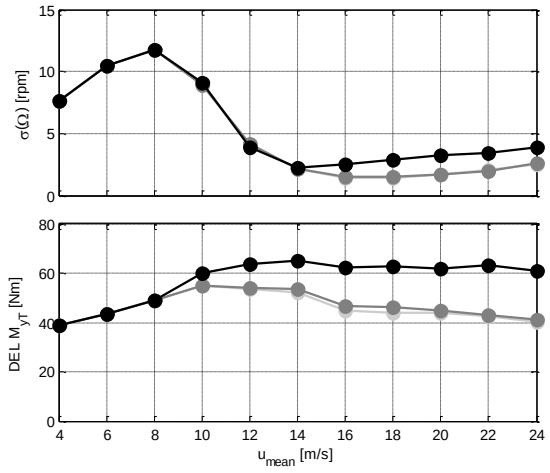

Figure 9: Average of standard deviation of the generator speed and lifetime weighted DEL of the tower base fore-aft bending moment for feedback controller only (black) and look-ahead controller (dark gray $\tau_{s,Spec}$, light gray τ_{Sim}).

Table 2: Lifetime weighted DEL of tower fore-aft bending moment for different controllers and prediction times.

Controller	DEL M_{yT} [MNm]	Changes to Σ_{FB}
Σ_{FB}	107.6	0%
$\Sigma_{FB} + \Sigma_{FFs}(\tau_{Sim})$	85.7	-20.4%
$\Sigma_{FB} + \Sigma_{FFs}(\tau_{s,Spec})$	86.9	-19.2%
$\Sigma_{FB} + \Sigma_{FFd}(\tau_{Sim})$	85.8	-20.3%
$\Sigma_{FB} + \Sigma_{FFd}(\tau_{d,Spec})$	86.9	-19.2%

Table 3: Reduction of lifetime weighted DEL of tower base fore-aft (m=4) and out-of-plane blade root bending moment (m=10) for the look-ahead controller for different wind distributions and wind turbine classes.

WT Class	A [m/s]	M_{yT}	M_{yB}
A	12	-20.4 %	-11.4%
	10	-15.8 %	-9.2 %
B	12	-19.5 %	-8.3 %
	10	-15.7 %	-6.1 %

6. Conclusion and Outlook

In this work a LIDAR simulator has been successfully coupled to GH Bladed. With this tool it was possible to evaluate the benefits of a LIDAR assisted collective pitch control in a realistic way by comparing it to the sophisticated UpWind controller.
The parameters of the controllers are optimized through the estimation of the generator speed spectra. The results show that best fatigue load reductions can be achieved for high turbulence and high wind speeds. In this region it is possible to reduce fatigue loads on tower and blades up to 20% and 10%, respectively. The static feedforward controller shows good robustness and no losses compared to a dynamic feedforward controller.
The LIDAR simulator will be improved and used to evaluate the benefit of LIDAR assisted control for extreme load reduction in a future work.

Acknowledgements

The presented work is part of the EU funded Research Project UpWind and of the BMU founded joint research project "Development of LIDAR technologies for the German offshore test field".

References

[1] Schlipf, D. and Kühn, M.: Prospects of a Collective Pitch Control by Means of Predictive Disturbance Compensation Assisted by Wind Speed Measurements, DEWEK, Bremen, Germany, 2008.
[2] Jonkman, J., Buttereld, S., Musial, W., and Scott, G.: Definition of a 5-MW reference wind turbine for offshore system development, National Renewable Energy Laboratory (NREL), Boulder, 2009.
[3] Bossanyi, E.: Controller for 5MW reference turbine, GH report 11593/BR/04, Bristol, 2009.
[4] IEC 61400-1 Ed. 3, Wind Turbines - Part 1: Design requirements, 2005.
[5] Veers, P.: Three-Dimensional Wind Simulation, Tech. rep., Sandia National Laboratories,1988.
[6] Schlipf, D., Trabucchi, D., Bischoff, O., Hofsäß, M., Mann, J., Mikkelsen, T., Rettenmeier, A., Trujillo, J.J., Kühn, M.: Testing of Frozen Turbulence Hypothesis for Wind Turbine Applications with a Scanning LIDAR System, ISARS, Paris, France, 2010.
[7] Lindelöw P.: Fiber Based Coherent Lidars for Remote Wind Sensing Ph.D. thesis, Danish Technical University, Copenhagen, Denmark, 2008.